Multibody System Dynamics **4:** 245–266, 2000.

Superelements Modelling in Flexible Multibody Dynamics

ALBERTO CARDONA
Centro Internacional de Métodos Computacionales en Ingeniería (CIMEC), INTEC – Universidad Nacional del Litoral/Conicet, Güemes 3450, 3000 Santa Fe, Argentina

(Received: 12 October 1999)

Abstract. We present a new implementation of substructuring methods for flexible multibody analysis. In previous developed formulations, we fixed the local axes of the superelement to one node. In this formulation, the reference frame is floating and close, in some sense, to the body center. The local frame is selected based on the positions of the interface nodes of the superelement, and completely independent of the order in which the nodes of the superelement are given. Therefore, the superelement itself depends only on the nodes positions, and on the mass and stiffness properties, thus allowing a very easy interfacing between the finite element program which computed the superelement and the mechanism analysis program.

Key words: multibody systems, nonlinear dynamics, mechanisms.

1. Introduction

Multibody dynamics problems are highly nonlinear, the nonlinearities being due to the large relative rotations between bodies. In fact, in many cases, the deformation effects inside each body are small enough to consider that its elastic behavior remains linear within a local frame. Then, we may say that in some sense, the nonlinearities are concentrated at the joints. This fact allows the development of sub-structuring methods for modeling complex elastic mechanism members based on the linear expansion of the elastic displacement field in a basis of deformation modes of the body.

The main advantage of substructuring techniques to describe flexible multibody systems is to allow the detailed modelling of components with complex geometry and structural function while keeping a relatively simple global dynamic model with a number of degrees of freedom as small as possible. The name *superelement* is used to denote the matrix model of the substructures treated using this technique.

These methods are based on the assumption that elastic effects are linear in a local frame relative to the body. Consequently, the concept of mechanical impedance/admittance, representing the dynamic behavior of any linear system ($\boldsymbol{S}$, $\boldsymbol{M}$), can be integrated within a modelization of articulated and flexible multibody structures. Each body is then represented by a superelement permitting to connect it

to its neighbours and containing the internal modal information. The so-called superelement consists of reduced stiffness and mass matrices coming, for instance, from a Craig and Bampton, Mac Neal or Rubin modal synthesis.

We assume a standard finite element software for structural analysis is available to perform first a modal analysis of the substructure under concern. The results from this analysis are the modal parameters in terms of which the superelement is constructed. However, superelement matrices can also be derived analytically or after identification from experimental measurements.

The flexible mechanism analysis software is used to perform the dynamic response analysis of the articulated system by coupling the superelement obtained in the previous step to the rest of the structure, the connection being achieved through a set of kinematic constraints at the attachment nodes. The degrees of freedom of the superelement are the translations and rotations at boundary nodes, plus the intensities of the internal modes to the model.

Several authors have proposed forms of substructuring methods for analyzing multibody systems [1, 11–18]. Most of them used vibration modes to model the dynamics of flexible multibodies with the limitation that the bodies are modeled by finite elements embedded in the mechanism analysis program. This paper is based on an implementation we have presented that elliminates this restriction [5, 7, 10]. Computation of the inertia terms is based on a co-rotational approximation of kinetic energy. It leads to a simple formulation and easy interfacing of the vibration analysis and dynamic response modules. The sole information transmitted from the vibration analysis module to build the superelement is the set of reduced stiffness and mass matrices.

Our previous formulation was based on building the local reference frame by attaching it to one node. This way of doing presents the inconvenience that when the user changes the location of the reference frame, results change (although slightly, if the hypothesis of small displacements is verified). Also, it was observed by experience that in most cases it is better, from the point of view of accuracy, to place the local frame close to the body center. In this paper, we are presenting a new formulation in which a floating local frame is defined based on the positions and rotations of the boundary nodes of the superelement. The origin of this local frame is placed as close as possible to the body center of mass. The characteristic of easy interfacing with the linear vibration analysis modules is retained, and the only information transmitted to the mechanism analysis program is, again, the set of reduced stiffness and mass matrices of the body.

The kinetic energy of the superelement is described using a corotational technique, as before. We analyze two different alternatives: a first technique, using angular velocities rotated to the local frame of the element, and a second one, in which the material angular velocities at each node of the boundary are used to construct the inertia terms. Examples have shown that, although the first alternative seems better since it is consistent with the treatment given to the translation velocities, the second alternative gave more accurate results.

Two examples of application are shown, illustrating the possibilities of the proposed technique.

2. The Component Mode Method in Dynamic Linear Analysis

The component mode method proposed by Craig and Bampton is based on a partitioning of the substructure degrees of freedom into *boundary degrees of freedom* $\boldsymbol{q}_B$ and *internal degrees of freedom* $\boldsymbol{q}_I$. The eigenvalue problem of the free-free substructure takes then the form

$$\begin{bmatrix} \boldsymbol{S}_{BB} & \boldsymbol{S}_{BI} \\ \boldsymbol{S}_{IB} & \boldsymbol{S}_{II} \end{bmatrix} \begin{Bmatrix} \boldsymbol{q}_B \\ \boldsymbol{q}_I \end{Bmatrix} = \omega^2 \begin{bmatrix} \boldsymbol{M}_{BB} & \boldsymbol{M}_{BI} \\ \boldsymbol{M}_{IB} & \boldsymbol{M}_{II} \end{bmatrix} \begin{Bmatrix} \boldsymbol{q}_B \\ \boldsymbol{q}_I \end{Bmatrix}. \tag{1}$$

The boundary modes $\boldsymbol{\Phi}_B$ are obtained by making the hypothesis that the internal DOF generate no inertia. They verify thus the approximate equation

$$\boldsymbol{S}_{IB}\boldsymbol{q}_B + \boldsymbol{S}_{II}\boldsymbol{q}_I \simeq 0, \tag{2}$$

hence the dependence relationship

$$\boldsymbol{q}_I = -\boldsymbol{S}_{II}^{-1}\boldsymbol{S}_{IB}\boldsymbol{q}_B, \tag{3}$$

which allows to construct the basis of boundary modes

$$\boldsymbol{\Phi}_B = \begin{bmatrix} \mathbf{1} \\ -\boldsymbol{S}_{II}^{-1}\boldsymbol{S}_{IB} \end{bmatrix}. \tag{4}$$

The internal vibration modes $\boldsymbol{\Phi}_I$ are next obtained by solving the internal eigenvalue problem of the substructure *clamped on its boundary*

$$\boldsymbol{S}_{II}\boldsymbol{q}_I = \omega^2 \boldsymbol{M}_{II}\boldsymbol{q}_I, \tag{5}$$

giving the eigensolutions $\{\omega_i^2, \boldsymbol{\phi}_{(i)}\}$. The matrix of internal modes is obtained by collecting the $m \ll NI$ first modes

$$\boldsymbol{\Phi}_I = \begin{bmatrix} \mathbf{0} \\ \boldsymbol{\phi}_{(1)}, \ldots, \boldsymbol{\phi}_{(m)} \end{bmatrix}. \tag{6}$$

The reduced stiffness and mass matrices of the superelement are then obtained by projecting the finite element stiffness and mass onto the basis formed by the sets of boundary and internal vibration modes.

3. Kinematic Hypotheses for a Superelement in Mechanism Analysis

The starting point consists to obtain the nodal positions and orientations through superposition of elastic displacements and rotations in a local frame convected with the rigid body motion of the substructure:

$$\begin{Bmatrix} \boldsymbol{x}_i \\ \boldsymbol{\Psi}_i \end{Bmatrix} = \begin{Bmatrix} \boldsymbol{x}_0 + \boldsymbol{R}_0(\boldsymbol{X}_i + \boldsymbol{u}_i) \\ \boldsymbol{\Psi}_0 \circ \boldsymbol{\psi}_i \end{Bmatrix} \tag{7}$$

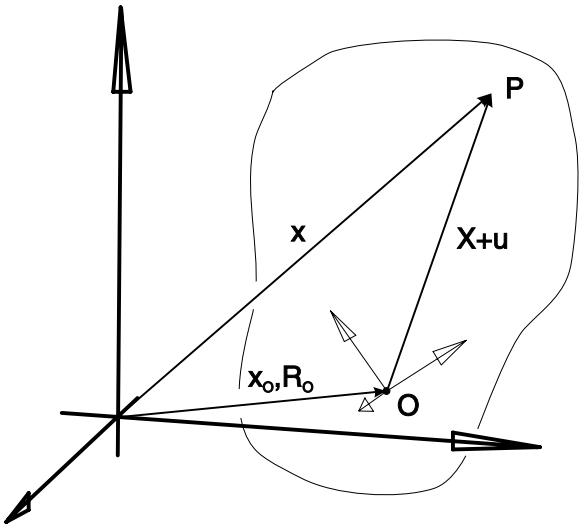

Figure 1. Flexible body kinematics.

with $\boldsymbol{x}_i$, $\boldsymbol{\Psi}_i$ the position and rotation vector of node i in the global frame, $\boldsymbol{x}_0$, $\boldsymbol{R}_0$ the position and rotation of the reference frame, $\boldsymbol{X}_i$ the initial position of node i in the local frame, $\boldsymbol{u}_i$, $\boldsymbol{\psi}_i$ the elastic displacements and rotations of node i in the local frame and $\circ$ the rotation composition operator [2, 3].

The hypothesis of infinitesimal elastic displacements and rotations in the local frame is made next:

$$\frac{\|\boldsymbol{u}_i\|}{\|\boldsymbol{X}_i\|}, \quad \|\boldsymbol{\psi}_i\| \ll 1. \tag{8}$$

The elastic displacements are expressed through superposition of component modes

$$\left\{ \begin{array}{c} \boldsymbol{x}_i \\ \boldsymbol{\Psi}_i \end{array} \right\} = \left\{ \begin{array}{c} \boldsymbol{x}_0 + \boldsymbol{R}_0(\boldsymbol{X}_i + \boldsymbol{\Phi}_i \boldsymbol{y}) \\ \boldsymbol{\Psi}_0 \circ (\boldsymbol{\Phi}_i \boldsymbol{y}) \end{array} \right\}, \tag{9}$$

where $\boldsymbol{\Phi}_i$ are the modal shape values evaluated at node i and $\boldsymbol{y}$ are the new generalized displacements.

The modal basis used is that obtained from the linear analysis:

$$\boldsymbol{\Phi}\ \boldsymbol{y} = \boldsymbol{\Phi}_B\ \boldsymbol{y}_B + \boldsymbol{\Phi}_I\ \boldsymbol{y}_I \tag{10}$$

with the boundary modes $\boldsymbol{\Phi}_B$ and the internal modes $\boldsymbol{\Phi}_I$ calculated from Equations (4) and (6).

In particular, the amplitudes of the constrained boundary modes may be expressed in the form

$$\boldsymbol{y}_B = \left\{ \begin{array}{c} \boldsymbol{u}_B \\ \boldsymbol{\psi}_B \end{array} \right\} = \left\{ \begin{array}{c} \boldsymbol{R}_0^T(\boldsymbol{x}_B - \boldsymbol{x}_0) - \boldsymbol{X}_B \\ (-\boldsymbol{\Psi}_0) \circ (\boldsymbol{\Psi}_B) \end{array} \right\}. \tag{11}$$

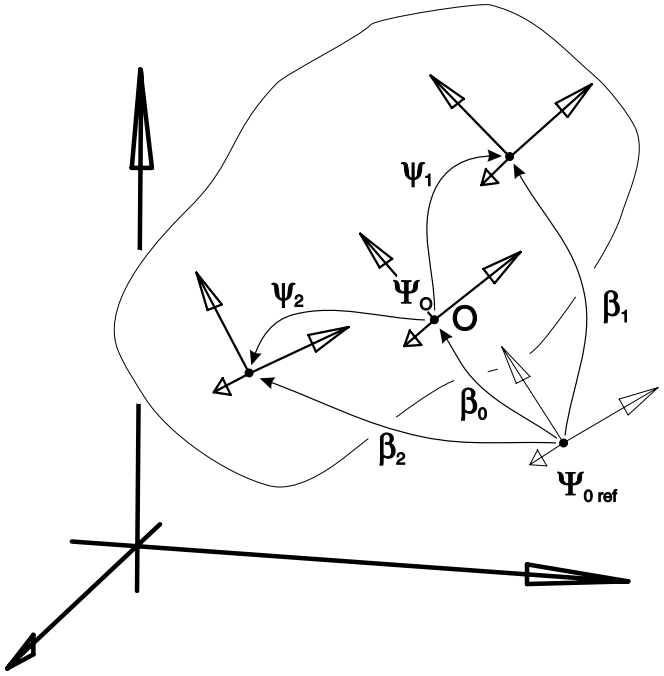

Figure 2. Construction of the local reference frame.

The superelement is built by using as generalized coordinates $\boldsymbol{q}$ the set of positions and rotations of the boundary nodes in the global frame, and the set of internal vibration modes

$$\boldsymbol{q}^T = \langle\, \boldsymbol{x}_B^T \quad \boldsymbol{\Psi}_{B\,\mathrm{inc}}^T \quad \boldsymbol{y}_I^T \,\rangle\,. \tag{12}$$

In fact, rotations at nodes are handled by an updated Lagrangian approach [2, 3], in which the current value is expressed as an increment with respect to a previously computed rotation:

$$\boldsymbol{\Psi}_i = \boldsymbol{\Psi}_{i\,\mathrm{ref}} \circ \boldsymbol{\Psi}_{i\,\mathrm{inc}}. \tag{13}$$

Subscripts 'ref' and 'inc' indicate nodal reference and increment rotation vectors, respectively. The nodal rotation unknowns are the increments with respect to the nodal reference rotation. This reference is updated after reaching convergence.

The position and orientation of the local frame is given in the form of a weighted mean of positions and orientations of the boundary nodes of the superelement. Position $\boldsymbol{x}_0$ will be computed as follows:

$$\boldsymbol{x}_0 = \sum_j \alpha_j \boldsymbol{x}_j, \tag{14}$$

where constant coefficients α_j are calculated as indicated below (Section 3.1).

In order to be able to compute a weighted mean of incremental rotations, we express them as increments with respect to a common reference frame. Let $\boldsymbol{\beta}_j$ be the rotation increment at node j, with respect to a common reference rotation $\boldsymbol{\Psi}_{0\,\mathrm{ref}}$:

$$\begin{aligned} \boldsymbol{\Psi}_0 &= \boldsymbol{\Psi}_{0\,\mathrm{ref}} \circ \boldsymbol{\beta}_0 \\ \boldsymbol{\Psi}_j &= \boldsymbol{\Psi}_{0\,\mathrm{ref}} \circ \boldsymbol{\beta}_j. \end{aligned} \tag{15}$$

The current orientation of the local frame of the superelement $\boldsymbol{\Psi}_0$ will be computed by requiring that

$$\boldsymbol{\beta}_0 = \sum_j \alpha_j \boldsymbol{\beta}_j. \tag{16}$$

The reference rotation vector $\boldsymbol{\Psi}_{0\,\mathrm{ref}}$ is selected as the rotation of the local frame in the previous converged configuration. After reaching convergence, this reference is updated and made equal to $\boldsymbol{\Psi}_0$.

Variations of local displacements and rotations are

$$\begin{aligned} \delta \boldsymbol{u}_i &= \boldsymbol{R}_0^T(\delta \boldsymbol{x}_i - \delta \boldsymbol{x}_0) + (\boldsymbol{R}_0^T(\boldsymbol{x}_i - \boldsymbol{x}_0)) \times \delta \boldsymbol{\Theta}_0, \\ \delta \boldsymbol{\psi}_i &= \boldsymbol{T}^{-1}(\boldsymbol{\psi}_i)(\delta \boldsymbol{\Theta}_i - \exp(\tilde{\boldsymbol{\psi}}_i)^T \delta \boldsymbol{\Theta}_0). \end{aligned} \tag{17}$$

Note that variations of positions and orientations of the reference frame can be expressed in terms of variations of positions and orientations at each boundary node:

$$\begin{aligned} \delta \boldsymbol{x}_0 &= \sum_j \alpha_j \delta \boldsymbol{x}_j, \\ \delta \boldsymbol{\beta}_0 &= \sum_j \alpha_j \delta \boldsymbol{\beta}_j. \end{aligned} \tag{18}$$

After replacing into Equation (17), we get

$$\begin{aligned} \delta \boldsymbol{u}_i &= \boldsymbol{R}_0^T \left(\delta \boldsymbol{x}_i - \sum_j \alpha_j \delta \boldsymbol{x}_j \right) \\ &\quad + (\boldsymbol{R}_0^T(\boldsymbol{x}_i - \boldsymbol{x}_0)) \boldsymbol{T}(\boldsymbol{\beta}_0) \sum_j \alpha_j \boldsymbol{T}^{-1}(\boldsymbol{\beta}_j) \delta \boldsymbol{\Theta}_j, \\ \delta \boldsymbol{\psi}_i &= \boldsymbol{T}^{-1}(\boldsymbol{\psi}_i) \delta \boldsymbol{\Theta}_i - \boldsymbol{T}^{-1}(\boldsymbol{\psi}_i) \exp(\tilde{\boldsymbol{\psi}}_i)^T \boldsymbol{T}(\boldsymbol{\beta}_0) \sum_j \alpha_j \boldsymbol{T}^{-1}(\boldsymbol{\beta}_j) \delta \boldsymbol{\Theta}_j. \end{aligned} \tag{19}$$

Finally, using the hypothesis of small rotation increments $\boldsymbol{\beta}_i$, $\boldsymbol{\psi}_i \ll 1$, we may write

$$\delta \boldsymbol{u}_i = \boldsymbol{R}_0^T \left((1 - \alpha_i) \delta \boldsymbol{x}_i - \sum_{j \neq i} \alpha_j \delta \boldsymbol{x}_j \right)$$

$$+ (\boldsymbol{R}_0^T(\boldsymbol{x}_i - \boldsymbol{x}_0)) \sum_j \alpha_j [2\mathbf{1} + \widetilde{\boldsymbol{\psi}}_j]/2 \, \delta\boldsymbol{\Theta}_j$$

$$\delta\boldsymbol{\psi}_i = [2(1-\alpha_i)\mathbf{1} + \widetilde{\boldsymbol{\psi}}_i]/2 \, \delta\boldsymbol{\Theta}_i - \sum_{j \neq i} \alpha_j [2\mathbf{1} + \widetilde{\boldsymbol{\psi}}_j - \widetilde{\boldsymbol{\psi}}_i]/2 \, \delta\boldsymbol{\Theta}_j. \quad (20)$$

3.1. COMPUTATION OF THE WEIGHT COEFFICIENTS $\boldsymbol{\alpha}$

Weights are computed from the mass and stiffness properties of the substructure. They express the form in which positions and rotations at the boundary nodes contribute to the reference frame global positioning and orientation. The choice for these coefficients is far from unique. From experience, we have found that the better option is one in which the reference frame corresponds, approximately, to a material frame located at the mass center of the substructure.

The algorithm we followed to compute the weights α is next described:

1. Compute the position of the center of mass $\boldsymbol{x}_{\text{cm}}$ from the stiffness and mass matrices of the superelement
2. Calculate weights α_i using

$$\boldsymbol{\alpha} = \text{pinv}(\boldsymbol{A})\boldsymbol{v}, \quad (21)$$

where matrix $\boldsymbol{A}$ and vector $\boldsymbol{v}$ are given by

$$\boldsymbol{A} = \begin{bmatrix} \boldsymbol{X}^T\boldsymbol{X} \\ \boldsymbol{e}^T \end{bmatrix}, \quad \boldsymbol{v} = \begin{Bmatrix} \boldsymbol{X}^T\boldsymbol{x}_{\text{cm}} \\ 1 \end{Bmatrix}, \quad (22)$$

and where $\boldsymbol{X} = [\boldsymbol{x}_1 \quad \boldsymbol{x}_2 \quad \ldots]$, $\boldsymbol{e}^T = \langle 1 \quad 1 \quad \ldots \rangle$, and $\text{pinv}(\boldsymbol{A})$ is the Moore–Penrose pseudoinverse of $\boldsymbol{A}$.

The computation of these weight factors through the Moore–Penrose pseudoinverse of $\boldsymbol{A}$ assures that (i) $\sum_i \alpha_i \boldsymbol{x}_i = \boldsymbol{x}_{\text{cm}}$ is verified in a least-squares sense, (ii) $\sum_i \alpha_i = 1$, and (iii) $\|\boldsymbol{\alpha}\|$ is minimum. Usually, all factors will have a non-zero contribution to the reference frame position and/or rotation.

Remark. Floating local frames coincident with the *current* principal axes, i.e. *Tisserand axes* [9] have the advantage of fully uncoupling the nonlinear inertia of the body. However, their use in flexible multibody dynamics requires a rather cumbersome algebraic manipulation and a full knowledge of the nonlinear matrices at the global level.

Remark. Note that different sets of weights can be defined for the positions and for the rotations, by considering the set of nodes that are retained in either case. The

only restriction is that the triplet of positions and/or rotations at the considered node should be included in the set of generalized displacements of the superelement.

Remark. Because of the particular form of the nonlinear kinematic relations between local and global variables (11), values at the boundaries should be given by triplets of positions and/or rotations at each node. Then, $\left\{ \begin{array}{c} \boldsymbol{x}_B \\ \boldsymbol{\Psi}_B \end{array} \right\}$ is in fact an abbreviate notation for:

$$\left\{ \begin{array}{c} \boldsymbol{x}_B \\ \boldsymbol{\Psi}_B \end{array} \right\} = \left\{ \begin{array}{cccc} \left\{ \begin{array}{c} \left\{ \begin{array}{c} \boldsymbol{x}_a \\ \boldsymbol{\Psi}_a \end{array} \right\} \\ \left\{ \begin{array}{c} \boldsymbol{x}_b \\ \boldsymbol{\Psi}_b \end{array} \right\} \\ \vdots \end{array} \right\}^T & \left\{ \begin{array}{c} \boldsymbol{x}_{ia} \\ \boldsymbol{x}_{ib} \\ \vdots \end{array} \right\}^T & \left\{ \begin{array}{c} \boldsymbol{\Psi}_{ja} \\ \boldsymbol{\Psi}_{jb} \\ \vdots \end{array} \right\}^T \end{array} \right\}^T . \tag{23}$$

Nodes $a, b, \ldots$ at the boundary have the six degrees of freedom defined. At nodes $ia, ib, \ldots$, only the translation degrees of freedom have been retained to build the superelement while at nodes $ja, jb, \ldots$, only the rotation degrees of freedom have been conserved.

4. Strain Energy and Internal Forces

Owing to the hypothesis of linear behavior in the local frame, the strain energy of the substructure may be written in the form

$$\pi = \frac{1}{2}\, \boldsymbol{y}^T \overline{\boldsymbol{S}} \boldsymbol{y} = \frac{1}{2} \left\{ \begin{array}{c} \boldsymbol{u}_B \\ \boldsymbol{\psi}_B \\ \boldsymbol{y}_I \end{array} \right\}^T \overline{\boldsymbol{S}} \left\{ \begin{array}{c} \boldsymbol{u}_B \\ \boldsymbol{\psi}_B \\ \boldsymbol{y}_I \end{array} \right\}, \tag{24}$$

where $\overline{\boldsymbol{S}}$ is the reduced stiffness obtained from the linear model

$$\overline{\boldsymbol{S}} = \boldsymbol{\Phi}^T \boldsymbol{S} \boldsymbol{\Phi} = \left[\begin{array}{cc} \overline{\boldsymbol{S}}_{BB} & \boldsymbol{0} \\ \boldsymbol{0} & \overline{\boldsymbol{S}}_{II} \end{array} \right]. \tag{25}$$

The variation of generalized displacements follows

$$\delta \boldsymbol{y} = \boldsymbol{\Upsilon}\, \delta \boldsymbol{q} = \left[\begin{array}{cc} \boldsymbol{\Upsilon}_B & \boldsymbol{0} \\ \boldsymbol{0} & \boldsymbol{1} \end{array} \right] \left\{ \begin{array}{c} \delta \boldsymbol{x}_B \\ \delta \boldsymbol{\Theta}_B \\ \boldsymbol{y}_I \end{array} \right\}, \tag{26}$$

where matrix $\boldsymbol{\Upsilon}_B$ reads

$$\boldsymbol{\Upsilon}_B = \left[\begin{array}{c} \boldsymbol{\Upsilon}_{1\,u} \\ \boldsymbol{\Upsilon}_{1\,\psi} \\ \boldsymbol{\Upsilon}_{2\,u} \\ \boldsymbol{\Upsilon}_{2\,\psi} \\ \vdots \end{array} \right], \tag{27}$$

and where matrices $\boldsymbol{\Upsilon}_{i\,u}$, $\boldsymbol{\Upsilon}_{i\,\psi}$ are computed from Equation (11) giving:

$$\boldsymbol{\Upsilon}_{i\,u} = \begin{bmatrix} -\alpha_1 \boldsymbol{R}_0^T & \alpha_1[\boldsymbol{R}_0^T \widetilde{(\boldsymbol{x}_1 - \boldsymbol{x}_0)}][2\mathbf{1} + \widetilde{\boldsymbol{\psi}}_1]/2 & \dots \\ (1-\alpha_i)\boldsymbol{R}_0^T & \alpha_i[\boldsymbol{R}_0^T \widetilde{(\boldsymbol{x}_i - \boldsymbol{x}_0)}][2\mathbf{1} + \widetilde{\boldsymbol{\psi}}_i]/2 & \dots \end{bmatrix}, \tag{28}$$

$$\boldsymbol{\Upsilon}_{i\,\psi} = \begin{bmatrix} \mathbf{0} & \alpha_1[2\mathbf{1} + \widetilde{\boldsymbol{\psi}}_1 - \widetilde{\boldsymbol{\psi}}_i]/2 & \dots \\ \mathbf{0} & [2(1-\alpha_i)\mathbf{1} + \widetilde{\boldsymbol{\psi}}_i]/2 & \dots \end{bmatrix}. \tag{29}$$

The superelement internal forces are obtained through variation of the strain energy

$$\delta\pi = \delta\boldsymbol{q} \cdot \boldsymbol{\Upsilon}^T \overline{\boldsymbol{S}}\boldsymbol{y} = \delta\boldsymbol{q} \cdot \boldsymbol{G}_{\text{int}}. \tag{30}$$

Finally, the tangent stiffness matrix is obtained through linearization of the internal forces

$$\Delta\boldsymbol{G}_{\text{int}} = \frac{\partial \boldsymbol{G}_{\text{int}}}{\partial \boldsymbol{q}} \cdot \Delta\boldsymbol{q} \simeq \boldsymbol{\Upsilon}^T \overline{\boldsymbol{S}} \boldsymbol{\Upsilon} \Delta\boldsymbol{q} = \overline{\boldsymbol{S}}_{\text{sup}} \Delta\boldsymbol{q}. \tag{31}$$

5. Kinetic Energy

The kinetic energy of the superelement is computed using the velocities rotated to the reference frame, in a corotational approach:

$$T = \frac{1}{2}\int_V \dot{\boldsymbol{x}} \cdot \dot{\boldsymbol{x}}\ \rho\ \mathrm{d}V = \frac{1}{2}\int_V (\boldsymbol{R}_0^T\dot{\boldsymbol{x}}) \cdot (\boldsymbol{R}_0^T\dot{\boldsymbol{x}})\ \rho\ \mathrm{d}V, \tag{32}$$

$\boldsymbol{R}_0$ gives the rotation of the reference frame.

We next compute the *discrete form* of the kinetic energy. Let us denote the velocities rotated to the reference frame by $\dot{\boldsymbol{x}}^*(\boldsymbol{X}) = \boldsymbol{R}_0^T\dot{\boldsymbol{x}}$ and interpolate them in terms of nodal velocities:

$$\dot{\boldsymbol{x}}^*(\boldsymbol{X}) = \sum_{i=1}^{n} N_i(\boldsymbol{X})\ \dot{\boldsymbol{x}}_i^* \tag{33}$$

where the summation extends to all nodes of the flexible member.

We have analyzed two different options for computing T. In the first one, angular velocities are consistently rotated to the reference frame in the form

$\boldsymbol{\Omega}^*(\boldsymbol{X}) = \boldsymbol{R}_0^T\boldsymbol{\omega}$, where $\boldsymbol{\omega}$ are (spatial) rotation velocities. After performing the volume integral, the kinetic energy of the superelement is written:

$$T = \frac{1}{2}\sum_i\sum_j \left\{ \begin{array}{c} \dot{\boldsymbol{x}}_i^* \\ \boldsymbol{\Omega}_i^* \end{array} \right\}^T \int_V \boldsymbol{N}_i^T \boldsymbol{N}_j \, \rho \, \mathrm{d}V \left\{ \begin{array}{c} \dot{\boldsymbol{x}}_j^* \\ \boldsymbol{\Omega}_j^* \end{array} \right\}$$

$$= \frac{1}{2}\sum_i\sum_j \left\{ \begin{array}{c} \dot{\boldsymbol{x}}_i^* \\ \boldsymbol{\Omega}_i^* \end{array} \right\}^T \boldsymbol{M}_{ij} \left\{ \begin{array}{c} \dot{\boldsymbol{x}}_j^* \\ \boldsymbol{\Omega}_j^* \end{array} \right\} \tag{34}$$

with $\boldsymbol{M}_{ij}$ the mass matrix block coupling nodes i and j. The second option consists into computing the kinetic energy in terms of material angular velocities, as it was already described in [5, 10] within the context of a node attached reference frame formulation. Now, the kinetic energy reads:

$$T = \frac{1}{2}\sum_i\sum_j \left\{ \begin{array}{c} \dot{\boldsymbol{x}}_i^* \\ \boldsymbol{\Omega}_i \end{array} \right\}^T \boldsymbol{M}_{ij} \left\{ \begin{array}{c} \dot{\boldsymbol{x}}_j^* \\ \boldsymbol{\Omega}_j \end{array} \right\}. \tag{35}$$

The first option gives a consistent treatment to both translation and rotation velocities. However, the second form of computing the kinetic energy gave us better accuracy, as it will be shown in the examples.

Remark. Note that the interpolation of velocities is not consistent with the interpolation of displacements used to build the strain energy expression.

6. Option A: Angular Velocities in the Reference Frame

The reduced form of the discrete kinetic energy (component modes approach) is next computed. First, a second stage discretization is made by assuming that the material velocities can be expressed in terms of a few global shape functions

$$\left\{ \begin{array}{c} \dot{\boldsymbol{x}}_i^* \\ \boldsymbol{\Omega}_i^* \end{array} \right\} = \boldsymbol{\Phi}_i \dot{\boldsymbol{y}} = \left[\, [\, \boldsymbol{\Phi}_{Bu} \quad \boldsymbol{\Phi}_{B\Psi} \,]_i \quad \boldsymbol{\Phi}_{I\,i} \, \right] \left\{ \begin{array}{c} \dot{\boldsymbol{x}}_B^* \\ \boldsymbol{\Omega}_B^* \\ \dot{\boldsymbol{y}}_I \end{array} \right\}, \tag{36}$$

where $\dot{\boldsymbol{x}}_B^*, \boldsymbol{\Omega}_B^*$ are the velocities at the boundary nodes of the superelement rotated to the reference frame, and $\dot{\boldsymbol{y}}_I$ are the time derivatives of the internal mode amplitudes.

By replacing into (34), the kinetic energy of the superelement T may be written as follows:

$$T = \frac{1}{2}\,\dot{\boldsymbol{y}}^T \overline{\boldsymbol{M}}\,\dot{\boldsymbol{y}} = \frac{1}{2} \left\{ \begin{array}{c} \dot{\boldsymbol{x}}_B^* \\ \boldsymbol{\Omega}_B^* \\ \dot{\boldsymbol{y}}_I \end{array} \right\}^T \overline{\boldsymbol{M}} \left\{ \begin{array}{c} \dot{\boldsymbol{x}}_B^* \\ \boldsymbol{\Omega}_B^* \\ \dot{\boldsymbol{y}}_I \end{array} \right\}. \tag{37}$$

The mass matrix $\overline{\boldsymbol{M}}$ results from the projection of the element mass matrices over the modal basis

$$\overline{\boldsymbol{M}} = \boldsymbol{\Phi}^T \boldsymbol{M} \boldsymbol{\Phi} = \begin{bmatrix} \overline{\boldsymbol{M}}_{BB} & \overline{\boldsymbol{M}}_{BI} \\ \overline{\boldsymbol{M}}_{IB} & \mathbf{1} \end{bmatrix}. \tag{38}$$

Remark. The vector of generalized velocities at the boundary $\begin{Bmatrix} \dot{\boldsymbol{x}}_B^* \\ \boldsymbol{\Omega}_B^* \end{Bmatrix}$ is in fact an abbreviate notation for:

$$\begin{Bmatrix} \dot{\boldsymbol{x}}_B^* \\ \boldsymbol{\Omega}_B^* \end{Bmatrix} = \left\{ \left\{ \begin{Bmatrix} \dot{\boldsymbol{x}}_a^* \\ \boldsymbol{\Omega}_a^* \end{Bmatrix} \begin{Bmatrix} \dot{\boldsymbol{x}}_b^* \\ \boldsymbol{\Omega}_b^* \end{Bmatrix} \vdots \right\}^T \quad \begin{Bmatrix} \dot{\boldsymbol{x}}_{ia}^* \\ \dot{\boldsymbol{x}}_{ib}^* \\ \vdots \end{Bmatrix}^T \quad \begin{Bmatrix} \boldsymbol{\Omega}_{ja}^* \\ \boldsymbol{\Omega}_{jb}^* \\ \vdots \end{Bmatrix}^T \right\}^T \tag{39}$$

in a consistent manner to what has already been pointed out in Section 3.1 before.

6.1. VARIATION OF KINETIC ENERGY AND INERTIA FORCES

The first variation of T is:

$$\delta T = \delta \dot{\boldsymbol{y}}^T \, \overline{\boldsymbol{M}} \, \dot{\boldsymbol{y}}. \tag{40}$$

The vector of variations of generalized velocities reads:

$$\delta \dot{\boldsymbol{y}} = \begin{Bmatrix} \delta \dot{\boldsymbol{x}}_B^* \\ \delta \boldsymbol{\Omega}_B^* \\ \delta \dot{\boldsymbol{y}}_I \end{Bmatrix} \tag{41}$$

with the variation of material and angular velocities

$$\begin{aligned} \delta \dot{\boldsymbol{x}}_B^* &= \boldsymbol{R}_0^T \delta \dot{\boldsymbol{x}}_B - \delta \boldsymbol{\Theta}_0 \times (\boldsymbol{R}_0^T \dot{\boldsymbol{x}}_B), \\ \delta \boldsymbol{\Omega}_B^* &= \boldsymbol{R}_0^T \boldsymbol{R}_B \delta \dot{\boldsymbol{\Theta}}_B - \delta \boldsymbol{\Theta}_0 \times \boldsymbol{R}_0^T \boldsymbol{R}_B \boldsymbol{\Omega}_B. \end{aligned} \tag{42}$$

The variation of the reference frame rotation can be computed in terms of variations of generalized displacements at the global frame giving:

$$\delta \boldsymbol{\Theta}_0 = \sum_i \alpha_i [2\mathbf{1} + \widetilde{\boldsymbol{\psi}}_i]/2 \, \delta \boldsymbol{\Theta}_i = \boldsymbol{U} \, \delta \boldsymbol{q}, \tag{43}$$

where matrix $\boldsymbol{U}$ is:

$$\boldsymbol{U} = [\, \mathbf{0} \quad \alpha_1 [2\mathbf{1} + \widetilde{\boldsymbol{\psi}}_1]/2 \quad \mathbf{0} \quad \alpha_2 [2\mathbf{1} + \widetilde{\boldsymbol{\psi}}_2]/2 \quad \dots \,]. \tag{44}$$

By introducing the latter expressions into (40) and by integrating by parts we get

$$\begin{aligned}\delta T &= -\delta \boldsymbol{q} \cdot \boldsymbol{G}_{\text{iner}} \\ &= -\delta \boldsymbol{q} \cdot \left(\boldsymbol{P}^T \, \overline{\boldsymbol{M}} \, \ddot{\boldsymbol{y}} + \boldsymbol{P}^T (\boldsymbol{O}_0 - \boldsymbol{O}_B) \overline{\boldsymbol{M}} \dot{\boldsymbol{y}} \right) + \delta \boldsymbol{\Theta}_0 \cdot \boldsymbol{V}^T \overline{\boldsymbol{M}} \dot{\boldsymbol{y}} \\ &= -\delta \boldsymbol{q} \cdot \left(\boldsymbol{P}^T \, \overline{\boldsymbol{M}} \, \ddot{\boldsymbol{y}} + \left(\boldsymbol{P}^T (\boldsymbol{O}_0 - \boldsymbol{O}_B) + \boldsymbol{U}^T \boldsymbol{V}^T \right) \overline{\boldsymbol{M}} \dot{\boldsymbol{y}} \right), \end{aligned} \tag{45}$$

where the local accelerations $\ddot{\boldsymbol{y}}$ are

$$\ddot{\boldsymbol{y}} = \left\{ \begin{array}{c} \boldsymbol{R}_0^T \ddot{\boldsymbol{x}}_B \\ \boldsymbol{R}_0^T \boldsymbol{R}_B \boldsymbol{A}_B \\ \ddot{\boldsymbol{y}}_I \end{array} \right\} + \left[\begin{array}{c} \widetilde{\dot{\boldsymbol{x}}}_B^* \\ \widetilde{\boldsymbol{\Omega}}_B^* \\ \boldsymbol{0} \end{array} \right] \boldsymbol{\Omega}_0 = \boldsymbol{P} \ddot{\boldsymbol{q}} + \boldsymbol{V} \boldsymbol{\Omega}_0, \tag{46}$$

and where

$$\begin{aligned} \boldsymbol{O}_0 &= \left[\begin{array}{ccc} \widetilde{\boldsymbol{\Omega}}_0 & & \\ & \widetilde{\boldsymbol{\Omega}}_0 & \\ & & \boldsymbol{0} \end{array} \right], \quad \boldsymbol{O}_B = \left[\begin{array}{ccc} \boldsymbol{0} & & \\ & \widetilde{\boldsymbol{\Omega}}_B^* & \\ & & \boldsymbol{0} \end{array} \right], \\ \boldsymbol{P} &= \left[\begin{array}{ccc} \boldsymbol{R}_0^T & & \\ & \boldsymbol{R}_0^T \boldsymbol{R}_B & \\ & & \boldsymbol{1} \end{array} \right], \quad \boldsymbol{V} = \left[\begin{array}{c} \widetilde{\dot{\boldsymbol{x}}}_B^* \\ \widetilde{\boldsymbol{\Omega}}_B^* \\ \boldsymbol{0} \end{array} \right]. \end{aligned} \tag{47}$$

6.2. TANGENT MASS AND PSEUDODAMPING MATRICES

The superelement tangent mass matrix is computed by differentiating the inertia forces with respect to the generalized accelerations in the global frame $\ddot{\boldsymbol{q}}$:

$$\overline{\boldsymbol{M}}_{\text{sup}} = \boldsymbol{P}^T \, \overline{\boldsymbol{M}} \, \boldsymbol{P}. \tag{48}$$

The inertia forces depend on the velocities $\dot{\boldsymbol{q}}$ – and, in fact, also on the generalized displacements $\boldsymbol{q}$. In order to improve convergence, we compute the matrix of derivatives of the inertia forces with respect to velocities, i.e. the superelement tangent pseudodamping matrix. This is a non symmetric matrix, which proved to be of great value for improving convergence in several examples.

$$\overline{\boldsymbol{C}}_{\text{sup}} = \underbrace{\overline{\boldsymbol{C}}_{1\,\text{sup}}}_{\text{symm}} + \underbrace{\overline{\boldsymbol{C}}_{2\,\text{sup}}}_{\text{skew}} + \overline{\boldsymbol{C}}_{3\,\text{sup}}, \tag{49}$$

where

$$\begin{aligned} \overline{\boldsymbol{C}}_{1\,\text{sup}} &= \boldsymbol{P}^T \left(\boldsymbol{O}_0 \overline{\boldsymbol{M}} + \overline{\boldsymbol{M}} \boldsymbol{O}_0^T \right) \boldsymbol{P}, \\ \overline{\boldsymbol{C}}_{2\,\text{sup}} &= \boldsymbol{P}^T \left(\overline{\boldsymbol{M}} \boldsymbol{V} + \boldsymbol{V}_1 \right) \boldsymbol{U} - \boldsymbol{U}^T \left(\boldsymbol{V}_1^T + \boldsymbol{V}^T \overline{\boldsymbol{M}} \right) \boldsymbol{P}^T, \\ \overline{\boldsymbol{C}}_{3\,\text{sup}} &= -\boldsymbol{P}^T \boldsymbol{O}_B \overline{\boldsymbol{M}} \boldsymbol{P} + \boldsymbol{P} \left[\begin{array}{ccc} \boldsymbol{0} & & \\ & \widetilde{(\overline{\boldsymbol{M}} \dot{\boldsymbol{y}})}_\Psi & \\ & & \boldsymbol{0} \end{array} \right], \end{aligned} \tag{50}$$

and where

$$\boldsymbol{V}_1 = \begin{bmatrix} \widetilde{(\overline{\boldsymbol{M}}\dot{\boldsymbol{y}})_x} \\ \widetilde{(\overline{\boldsymbol{M}}\dot{\boldsymbol{y}})_\psi} \\ \boldsymbol{0} \end{bmatrix}. \tag{51}$$

7. Option B: Angular Velocities in the Material Frame

In this case, the second stage discretization applies to the material angular velocities instead of the reference frame angular velocities:

$$\begin{Bmatrix} \dot{\boldsymbol{x}}_i^* \\ \boldsymbol{\Omega}_i \end{Bmatrix} = \boldsymbol{\Phi}_i \dot{\boldsymbol{y}} = \begin{bmatrix} [\,\boldsymbol{\Phi}_{Bu} \quad \boldsymbol{\Phi}_{B\Psi}\,]_i & \boldsymbol{\Phi}_{I\,i} \end{bmatrix} \begin{Bmatrix} \dot{\boldsymbol{x}}_B^* \\ \boldsymbol{\Omega}_B \\ \dot{\boldsymbol{y}}_I \end{Bmatrix} \tag{52}$$

with $\dot{\boldsymbol{x}}_B^*$, $\boldsymbol{\Omega}_B$ the velocities at the boundary nodes of the superelement, the former rotated to the reference frame and the latter terms expressed in the material frame.

By replacing into (35), the kinetic energy of the superelement T may be written as follows:

$$T = \frac{1}{2}\,\dot{\boldsymbol{y}}^T \overline{\boldsymbol{M}}\,\dot{\boldsymbol{y}} = \frac{1}{2} \begin{Bmatrix} \dot{\boldsymbol{x}}_B^* \\ \boldsymbol{\Omega}_B \\ \dot{\boldsymbol{y}}_I \end{Bmatrix}^T \overline{\boldsymbol{M}} \begin{Bmatrix} \dot{\boldsymbol{x}}_B^* \\ \boldsymbol{\Omega}_B \\ \dot{\boldsymbol{y}}_I \end{Bmatrix} \tag{53}$$

with the mass matrix $\overline{\boldsymbol{M}}$ given by the projection of the global mass matrix over the modal basis (38). Again, the vector of generalized velocities at the boundary $\begin{Bmatrix} \dot{\boldsymbol{x}}_B^* \\ \boldsymbol{\Omega}_B \end{Bmatrix}$ is an abbreviate notation for the whole set of velocities at the boundary, as pointed out in (39).

7.1. VARIATION OF KINETIC ENERGY AND INERTIA FORCES

The first variation of T reads:

$$\delta T = \delta \dot{\boldsymbol{y}}^T\, \overline{\boldsymbol{M}}\, \dot{\boldsymbol{y}} \tag{54}$$

with the vector of variations of generalized velocities:

$$\delta \dot{\boldsymbol{y}} = \begin{Bmatrix} \delta \dot{\boldsymbol{x}}_B^* \\ \delta \boldsymbol{\Omega}_B \\ \delta \dot{\boldsymbol{y}}_I \end{Bmatrix} \tag{55}$$

and with the variations

$$\begin{aligned} \delta \dot{\boldsymbol{x}}_B^* &= \boldsymbol{R}_0^T \delta \dot{\boldsymbol{x}}_B - \delta \boldsymbol{\Theta}_0 \times (\boldsymbol{R}_0^T \dot{\boldsymbol{x}}_B), \\ \delta \boldsymbol{\Omega}_B &= \delta \dot{\boldsymbol{\Theta}}_B - \delta \boldsymbol{\Theta}_B \times \boldsymbol{\Omega}_B. \end{aligned} \tag{56}$$

By introducing the latter expressions into (54), together with the expression of variations of the reference frame rotation (43), and by integrating by parts between two arbitrary time instants (Hamilton principle), we get

$$\begin{aligned}\delta T &= -\delta \boldsymbol{q} \cdot \boldsymbol{G}_{\text{iner}},\\ &= -\delta \boldsymbol{q} \cdot (\boldsymbol{P}^T\, \overline{\boldsymbol{M}}\, \ddot{\boldsymbol{y}} + \boldsymbol{P}^T(\boldsymbol{O}_0 + \boldsymbol{O}_B)\overline{\boldsymbol{M}}\dot{\boldsymbol{y}}) + \delta \boldsymbol{\Theta}_0 \cdot \boldsymbol{V}^T \overline{\boldsymbol{M}}\dot{\boldsymbol{y}},\\ &= -\delta \boldsymbol{q} \cdot \left(\boldsymbol{P}^T\, \overline{\boldsymbol{M}}\, \ddot{\boldsymbol{y}} + (\boldsymbol{P}^T(\boldsymbol{O}_0 + \boldsymbol{O}_B) + \boldsymbol{U}^T \boldsymbol{V}^T)\overline{\boldsymbol{M}}\dot{\boldsymbol{y}}\right), \end{aligned} \tag{57}$$

where the local accelerations $\ddot{\boldsymbol{y}}$ are

$$\ddot{\boldsymbol{y}} = \left\{ \begin{array}{c} \boldsymbol{R}_0^T \ddot{\boldsymbol{x}}_B \\ \boldsymbol{A}_B \\ \ddot{\boldsymbol{y}}_I \end{array} \right\} + \begin{bmatrix} \widetilde{\ddot{\boldsymbol{x}}}_B^* \\ \boldsymbol{0} \\ \boldsymbol{0} \end{bmatrix} \boldsymbol{\Omega}_0 = \boldsymbol{P}\ddot{\boldsymbol{q}} + \boldsymbol{V}\boldsymbol{\Omega}_0, \tag{58}$$

and where matrices $\boldsymbol{O}_0$, $\boldsymbol{O}_B$, $\boldsymbol{P}$ and $\boldsymbol{V}$ are given, in this option, by the expressions:

$$\begin{aligned} \boldsymbol{O}_0 &= \begin{bmatrix} \widetilde{\boldsymbol{\Omega}}_0 & & \\ & \boldsymbol{0} & \\ & & \boldsymbol{0} \end{bmatrix}, \quad \boldsymbol{O}_B = \begin{bmatrix} \boldsymbol{0} & & \\ & \widetilde{\boldsymbol{\Omega}}_B & \\ & & \boldsymbol{0} \end{bmatrix},\\ \boldsymbol{P} &= \begin{bmatrix} \boldsymbol{R}_0^T & & \\ & \boldsymbol{1} & \\ & & \boldsymbol{1} \end{bmatrix}, \quad \boldsymbol{V} = \begin{bmatrix} \widetilde{\dot{\boldsymbol{x}}}_B^* \\ \boldsymbol{0} \\ \boldsymbol{0} \end{bmatrix}. \end{aligned} \tag{59}$$

7.2. TANGENT MASS AND PSEUDODAMPING MATRICES

After differentiating the inertia forces with respect to the generalized accelerations in the global frame $\ddot{\boldsymbol{q}}$, we get the tangent mass matrix of the superelement:

$$\overline{\boldsymbol{M}}_{\text{sup}} = \boldsymbol{P}^T\, \overline{\boldsymbol{M}}\, \boldsymbol{P}. \tag{60}$$

The inertia forces also depend on the generalized velocities $\dot{\boldsymbol{q}}$ and displacements $\boldsymbol{q}$. In order to improve convergence, it is necessary to compute the matrix of derivatives of the inertia forces with respect to velocities, i.e. the superelement tangent pseudodamping matrix.

$$\overline{\boldsymbol{C}}_{\text{sup}} = \underbrace{\overline{\boldsymbol{C}}_{1\,\text{sup}}}_{\text{symm}} + \underbrace{\overline{\boldsymbol{C}}_{2\,\text{sup}}}_{\text{skew}} + \overline{\boldsymbol{C}}_{3\,\text{sup}}, \tag{61}$$

where

$$\begin{aligned} \overline{\boldsymbol{C}}_{1\,\text{sup}} &= \boldsymbol{P}^T \left(\boldsymbol{O}_0 \overline{\boldsymbol{M}} + \overline{\boldsymbol{M}} \boldsymbol{O}_0^T\right) \boldsymbol{P},\\ \overline{\boldsymbol{C}}_{2\,\text{sup}} &= \boldsymbol{P}^T \left(\overline{\boldsymbol{M}}\boldsymbol{V} + \boldsymbol{V}_1\right) \boldsymbol{U} - \boldsymbol{U}^T \left(\boldsymbol{V}_1^T + \boldsymbol{V}^T \overline{\boldsymbol{M}}\right) \boldsymbol{P}^T,\\ \overline{\boldsymbol{C}}_{3\,\text{sup}} &= \boldsymbol{O}_B \overline{\boldsymbol{M}} \boldsymbol{P} - \begin{bmatrix} \boldsymbol{0} & \widetilde{(\overline{\boldsymbol{M}}\dot{\boldsymbol{y}})_\Psi} & \\ & & \boldsymbol{0} \end{bmatrix}, \end{aligned} \tag{62}$$

and where

$$\boldsymbol{V}_1 = \begin{bmatrix} \widetilde{(\overline{\boldsymbol{M}}\dot{\boldsymbol{y}})_x} \\ \boldsymbol{0} \\ \boldsymbol{0} \end{bmatrix}. \tag{63}$$

Remark. In both options A and B, all contributions to the inertia terms (inertia forces $\boldsymbol{G}_{\text{iner}}$, mass matrix $\overline{\boldsymbol{M}}_{\text{sup}}$ and pseudodamping matrix $\overline{\boldsymbol{C}}_{\text{sup}}$) are evaluated directly from the reduced mass matrix $\overline{\boldsymbol{M}}$. In this way, we can very easily interface the vibration analysis code and the mechanism analysis module. This represents a great advantage with respect to other techniques, as that we presented earlier in [6].

8. Examples

The equations of motion we get by following the techniques described in the preceding sections were time-integrated using a particular implementation of the Hilber–Hughes–Taylor algorithm to solve flexible mechanisms problems. This implementation of the HHT integrator was particularly adapted to treat large finite rotations and equations of constraint, and is fully described in [4, 8].

8.1. HINGED BEAM

The first example is a hinged flexible beam, initially at rest, submitted to a time-varying torque at its base. The beam is linked to the foundation through a hinge joint (Figure 3). Its physical properties are: length 141.42, mass density 7.8×10^{-3}, cross section 9.0, moment of inertia 6.75, Young modulus 2.1×10^6 and Poisson ratio 0.3. All computations were made with a time step $\Delta t = 0.01$.

The dynamic response was computed using a reduced model in which translations and rotations are retained at the two extremes of the beam, and four internal vibration modes are included, resulting in a 16 degrees-of-freedom model. Results were compared to those of a model formed by five equally-spaced nonlinear beam finite elements, described in [3]. We have also made computations using a superelement with a node-attached local reference frame, as described in [5].

Figure 4 shows results computed with the node-attached reference frame formulation. We compare results obtained when changing the reference node; i.e. in one case the node at the base of the beam was used to attach the reference frame and in the second case the node at the tip was used for this purpose. We see that results in both cases, although similar, differ from each other.

In Figure 5 we compare one of the solutions of the node-attached formulation with the solution obtained by integrating the nonlinear beam finite element model. We can appreciate that the reduced model results are enough accurate for practical purposes.

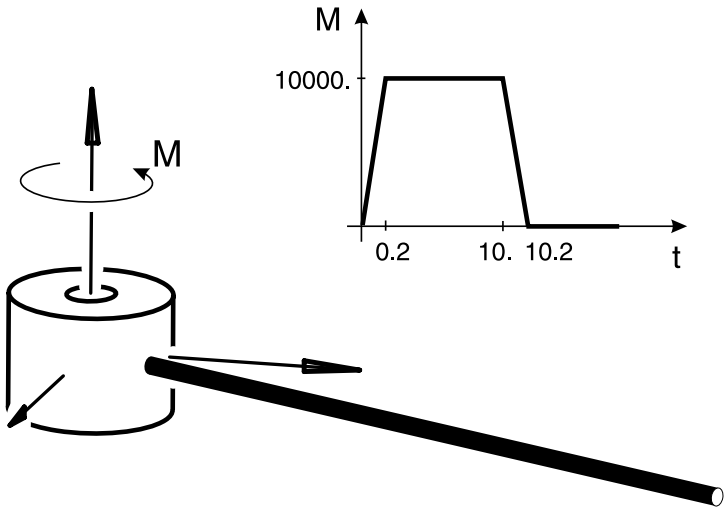

Figure 3. Hinged beam.

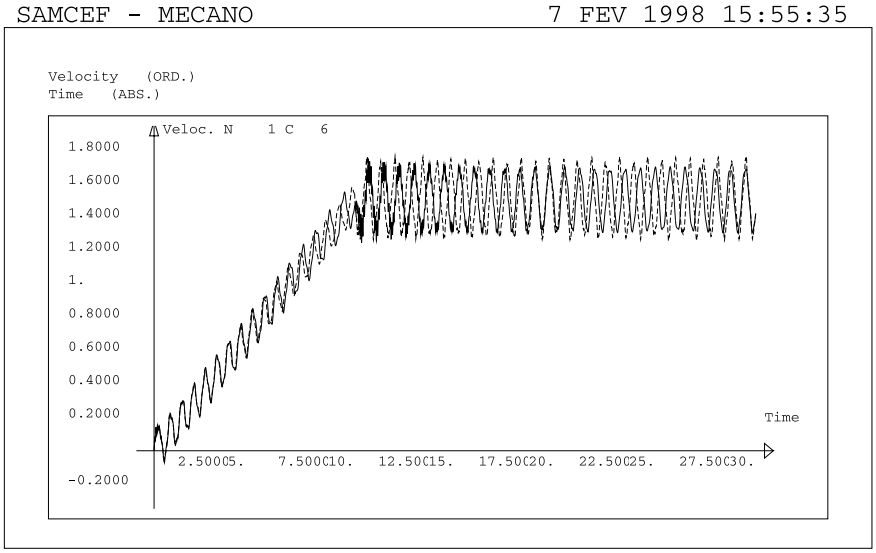

Figure 4. Hinged beam. Time evolution of the angular velocity at the base of the beam. Results obtained when changing the reference node in the node-attached reference frame formulation.

In Figures 6 and 7 we display the time evolution of the angular velocity at the base node of the beam computed with the new formulation presented here, for both options A and B of computing the kinetic energy. They are again compared to the nonlinear beams finite element solution. We can appreciate an accurate computed response in both reduced models. The solution is slightly more accurate than the solution computed using the attached-node formulation. We should remark that

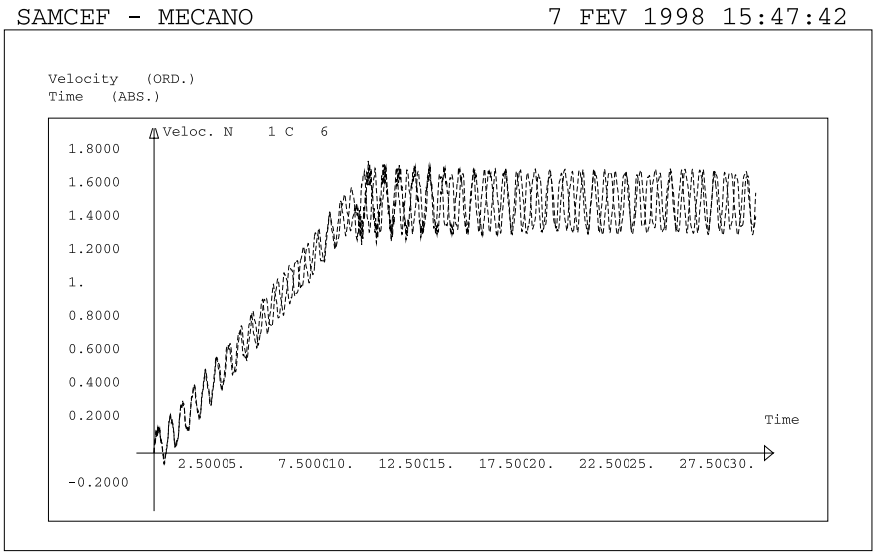

Figure 5. Hinged beam. Angular velocity at the base of the beam. Results obtained with the node-attached reference frame formulation (reference at the base of the beam) compared to the nonlinear beam finite element solution.

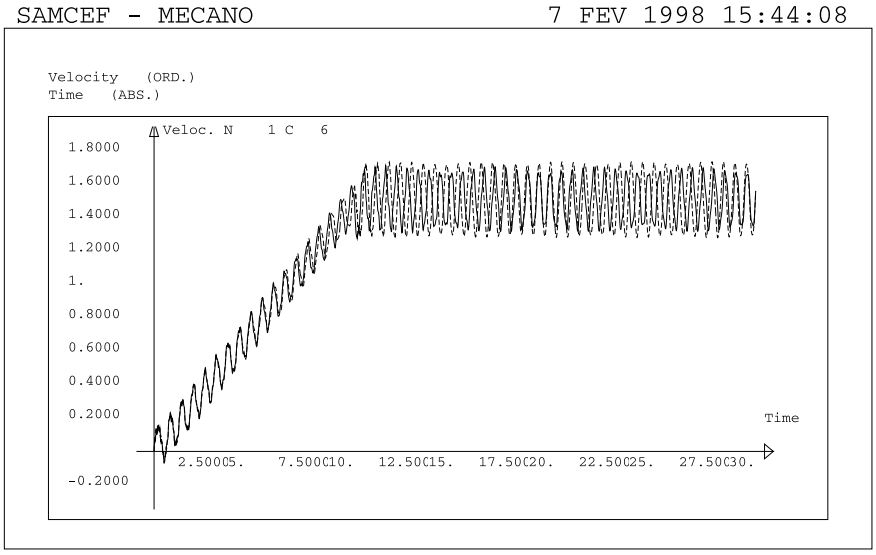

Figure 6. Hinged beam. Angular velocity at the base of the beam. Results obtained with the floating reference frame formulation, inertia option A, compared to the nonlinear beam finite element solution.

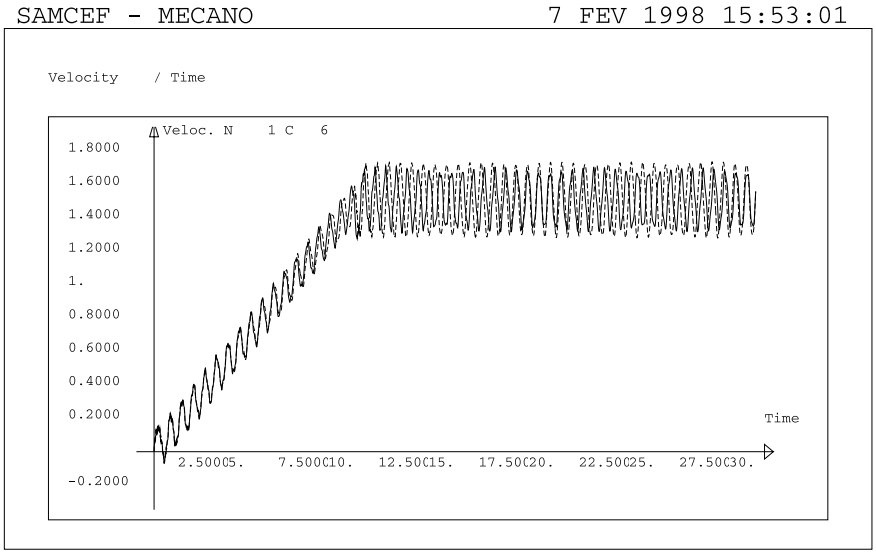

Figure 7. Hinged beam. Angular velocity at the base of the beam. Results obtained with the floating reference frame formulation, inertia option B, compared to the nonlinear beam finite element solution.

this formulation is completely invariant with respect to the order given to the superelement nodes, a fact verified also by computations.

8.2. BEAM ON A SPHERICAL JOINT

This second example is again a flexible beam articulated to the foundation. In this case, the beam is linked through a spherical joint to the ground and a vertical impulse is applied at time $t = 15$ in order to get full three-dimensional motion (Figure 8). Physical data coincide with those of the first example. Now, computations were made with a time step $\Delta t = 0.02$. This example is intended to compare results given by both forms of computing the inertia terms in the floating reference frame formulation.

The reduced model was again built by retaining translations and rotations at the two extremes of the beam, and by including four internal vibration modes. Results were compared to those of a five equally-spaced nonlinear beam finite elements model.

Figure 9 displays the z-angular velocity computed using the node-attached reference frame formulation. On the other hand, Figures 10 and 11 show the results of computations using both options for computing the inertia terms in the floating reference frame formulation. In all cases, the responses are compared to that of the nonlinear beams model. We can see that results are almost identical in all cases, up to the time instant in which the vertical impulse is applied. Afterwards, the response

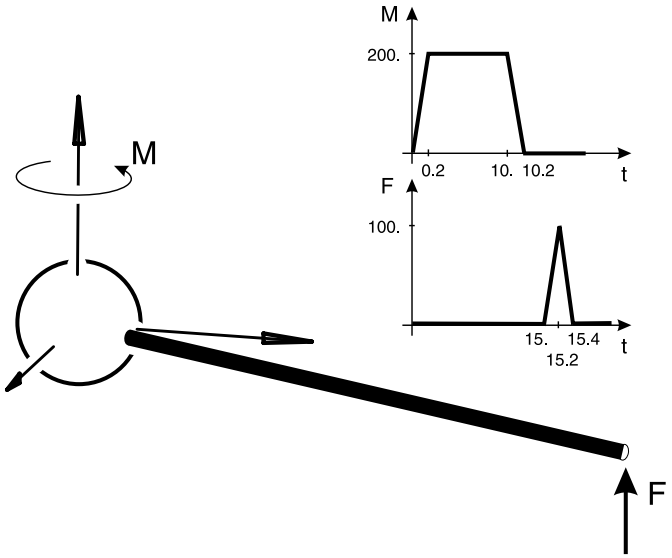

Figure 8. Beam on a spherical joint.

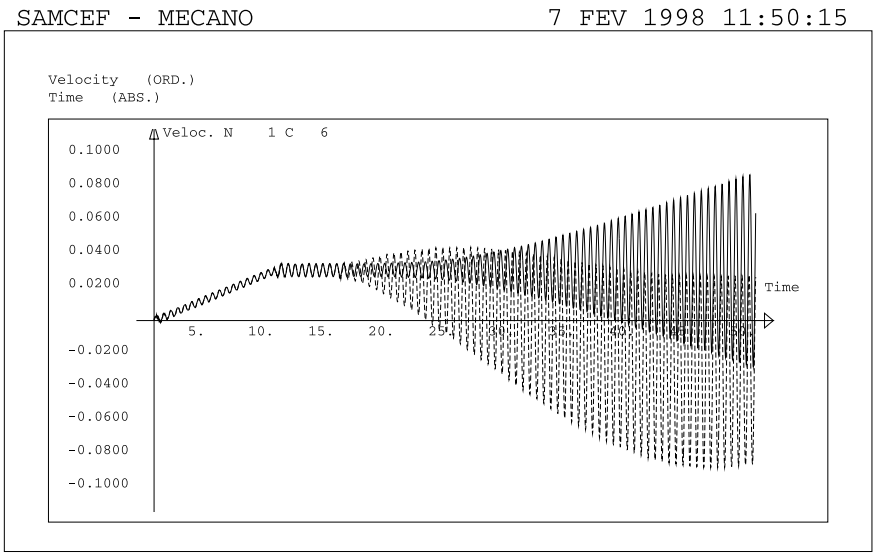

Figure 9. Beam on spherical joint. Angular velocity at the base of the beam. Results obtained with the node-attached reference frame formulation, compared to the nonlinear beam finite element solution.

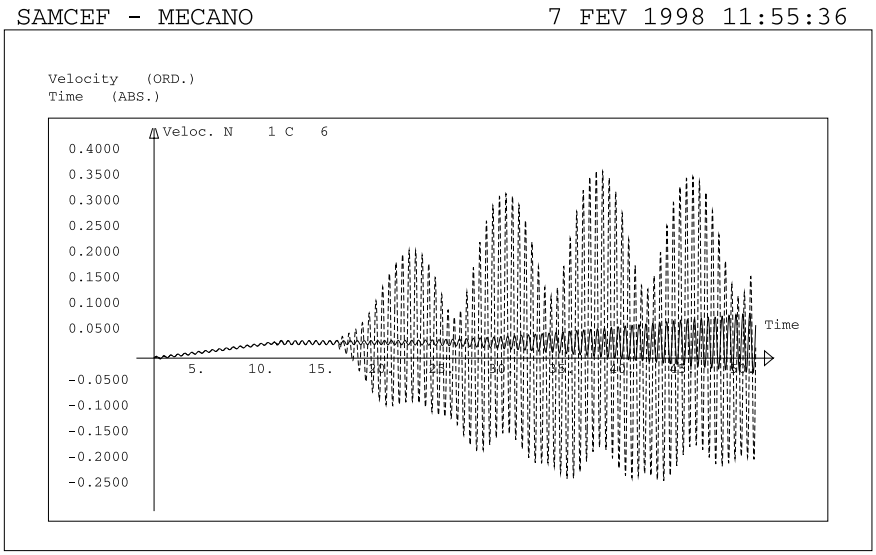

Figure 10. Beam on spherical joint. Angular velocity at the base of the beam. Results obtained with the floating reference frame formulation, inertia option A, compared to the nonlinear beam finite element solution.

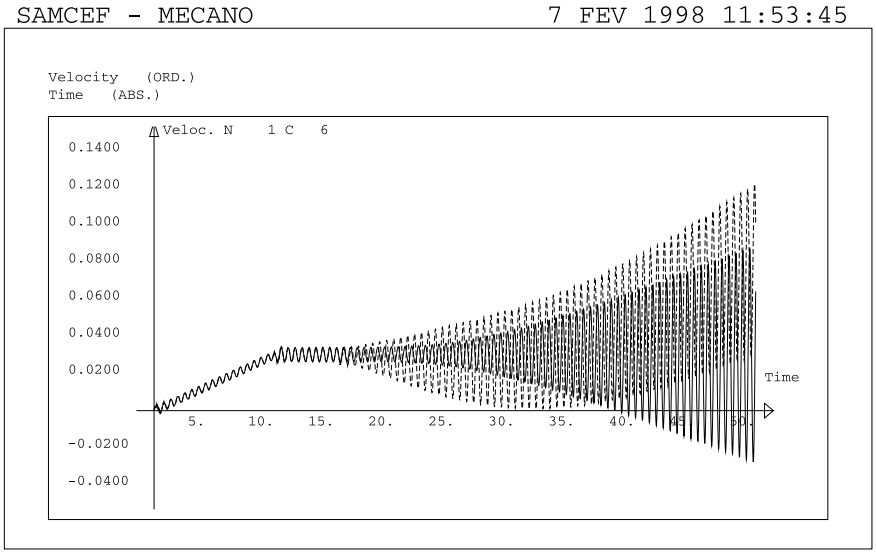

Figure 11. Beam on spherical joint. Angular velocity at the base of the beam. Results obtained with the floating reference frame formulation, inertia option B, compared to the nonlinear beam finite element solution.

computed using option A of the kinetic energy presents large amplitude spurious oscillations. The node-attached formulation and the floating reference frame formulation (option B), display similar behaviors comparing well to the results of the nonlinear beam finite element model. We remark again a slightly better accuracy in the floating frame formulation, option B, than in the node-attached formulation.

9. Concluding Remarks

A new formulation of a superelement for flexible mechanisms analysis has been presented. This formulation is based on using a floating reference frame and a corotational inertia approach. The floating reference frame presents a better way of modeling flexible bodies than with the fixed reference frame approach, since results are completely independent of the choice of reference frame node. Also, with the corotational inertia approach, the formulation allows to very easily interface the mechanisms analysis program with the linear vibrations analysis module.

Two different alternatives of computing the kinetic energy have been proposed and compared. In the first alternative, angular velocities in the reference frame are used to evaluate the kinetic energy while the second one uses angular velocities expressed in the material frame for this purpose. Although the former alternative is consistent to the treatment given to the traslation velocities, the latter gave more accurate results.

The floating reference frame position and orientation is built in terms of the boundary nodes positions and rotations (and on the mass properties). Forthcoming work will be directed to allow constructing a floating reference frame uniquely in terms of boundary nodes positions.

References

1. Agrawal, O. and Shabana, A., 'Application of deformable-body mean axis to flexible multibody system dynamics', *Comput. Methods Appl. Mech. Engrg.* **56**, 1986, 217–245.
2. Cardona, A., 'An integrated approach to mechanism analysis', Ph.D. Thesis, Faculté des Sciences Appliquées, Université de Liège, 1989.
3. Cardona, A. and Géradin, M., 'A beam finite element nonlinear theory with finite rotations', *Internat. J. Numer. Methods Engrg.* **26**, 1988, 2403–2438.
4. Cardona, A. and Géradin, M., 'Time integration of the equations of motion in mechanism analysis', *Comput. & Structures* **33**, 1989, 801–820.
5. Cardona, A. and Géradin, M., 'Modeling of superelements in mechanism analysis', *Internat. J. Numer. Methods Engrg.* **32**, 1991, 1565–1593.
6. Cardona, A. and Géradin, M., 'A superelement formulation for mechanism analysis', *Comput. Methods Appl. Mech. Engrg.* **100**, 1992, 1–29.
7. Cardona, A. and Géradin, M., 'Flexible multibody analysis using impedance and/or admittance models', in *Mecánica Computacional Vol. XIV, Anales IV Congreso Argentino de Mecánica Computacional*, Mar del Plata, Argentina, 1994, 638–645.
8. Cardona, A. and Géradin, M., 'Numerical integration of second-order differential-algebraic systems in flexible mechanism dynamics', in *Computer-Aided Analysis of Rigid and Flexible*

Mechanical Systems, M.S. Pereira and J. Ambrosio (eds.), NATO ASI Series E268, Kluwer Academic Publishers, Dordrecht, 1994, 501–529.
9. de Veubeke, B.F., 'The dynamics of flexible bodies', *Internat. J. Engrg. Sci.* **14**, 1976, 895–913.
10. Géradin, M. and Cardona, A., 'Substructuring techniques in flexible multibody systems', in *Eight VPI & SU Symposium on Dynamics and Control of Large Space Structures*, 1991.
11. Shabana, A., 'Substructure synthesis methods for dynamic analysis of multi-body systems', *Comput. & Structures* **20**, 1985, 737–744.
12. Shabana, A., *Dynamics of Multibody Systems*, John Wiley & Sons, New York, 1989.
13. Shabana, A., 'Flexible multibody dynamics: Review of past and recent developments', *Multibody Systems Dynamics* **1**, 1997, 189–222.
14. Shabana, A. and Wehage, R., 'A coordinate reduction technique for dynamic analysis of spatial substructures with large angular rotations', *J. Structural Mech.* **11**, 1983, 401–431.
15. Walrapp, O., 'Linearized flexible multibody dynamics including geometric stiffening effects', *Internat. J. Mech. Structures Mach.* **19**, 1991, 385–409.
16. Wu, S. and Haug, E., 'Geometric nonlinear substructuring for dynamics of flexible mechanical systems', *Internat. J. Numer. Methods Engrg.* **26**, 1988, 2211–2226.
17. Yoo, W. and Haug, E., 'Dynamics of articulated structures. Part I. Theory', *J. Structural Mech.* **14**, 1986, 105–126.
18. Yoo, W. and Haug, E., 'Dynamics of articulated structures. Part II. Computer implementation and applications', *J. Structural Mech.* **14**, 1986, 177–189.